Tunable Filters Based on Cascaded Long-Period Polymer Waveguide Gratings

Xin SHI, Rui CAO, and Lingfang WANG*

School of Optoelectronic Science and Engineering, University of Electronic Science and Technology of China, Chengdu 611731, China

*Corresponding author: Lingfang WANG E-mail: lf.wang@uestc.edu.cn

Abstract: Long-period waveguide grating based filters have attracted attention due to their flexible fabrication, a variety of materials and structures, low back reflection, low insertion loss, and excellent performance in the tuning range and temperature sensitivity. To our knowledge, for the first time, a two-segment polymer long-period waveguide grating was cascaded to implement a filter with a narrower bandwidth. Experimental results showed that the device had a maximum extinction ratio of 24 dB at 1577 nm, and the 12 dB bandwidth was 10 nm. The temperature sensitivity of the fabricated device was 1.79 nm/℃.

Keywords: Long-period waveguide grating; optical waveguide; mode coupling; filter

Citation: Xin SHI, Rui CAO, and Lingfang WANG, "Tunable Filters Based on Cascaded Long-Period Polymer Waveguide Gratings," *Photonic Sensors*, 2022, 12(4): 220415.

1. Introduction

Long-period gratings (LPGs), generally refer to gratings with a grating period of tens to hundreds of microns, including long-period fiber gratings (LPFGs) and long-period waveguide gratings (LPWGs) [1, 2]. Compared with long-period Bragg gratings, which are mainly used for reverse transmission coupling conversion, LPFGs are easier to transfer modes in the same direction with the simple fabrication process, low reverse reflection, and suitable tuning wavelength [3].

LPWGs based on polymer materials can make full use of the advantages of low cost, ease to fabricate waveguides on different substrates and end faces, high thermal-optical coefficient, low dielectric constant, fast response time, adjustable refractive index, etc., to achieve more sensitive wavelength selection [4]. It greatly promotes the research of various applications of LPWGs such as the mode division multiplexer, refractive index sensor, and mode converter [5–11].

In this paper, we proposed a strategy to enhance the device wavelength selectivity by cascading two segments of long-period waveguides (LWGs) to realize a filter with the narrower bandwidth. Our proposed device with the simple manufacturing process worked based on two core modes in a multimode waveguide. Experimental results showed that the device resonance wavelength was 1577 nm, the maximum extinction ratio was 24 dB, the 12 dB bandwidth was 10 nm, and the temperature sensitivity was 1.79 nm/℃.

2. Theory

We fabricated two LPWGs with the same period on one multimode waveguide, as shown in Fig. 1. The pump laser launched from the input facet was

Received: 15 April 2021 / Revised: 9 January 2022

DOI: 10.1007/s13320-022-0659-4
Article type: Regular

transmitted in the waveguide core in the form of the fundamental mode (A) and was partially coupled to a higher-order mode (B) after passing through the LPWG1 according to the phase matching equation $(\beta_{01}-\beta_{0m})\Lambda=2\pi$, where β_{01} and β_{0m} represent the propagation constant of the fundamental mode and higher-order mode, and Λ is the grating period.

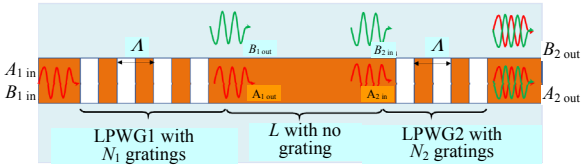

Fig. 1 Schematic diagram of the cascaded LPWG structure.

The higher-order mode (B) and the remaining fundamental mode (A) transmitted in the waveguide layer independently. By reasonably designing the distance (L) between the two LPWGs, a phase difference π was generated after transmission. At LPWG2, the high-order mode was re-coupled and converted to a fundamental core mode. Due to the π phase difference, interference cancellation occurred between the two fundamental modes, which narrowed the stopband bandwidth of the transmission spectrum.

The transfer matrix method was used to analyze the proposed structure. The LWG what we set was uniform, so that the mode coupling amount C and the phase shift φ caused by each periodic grating were the same. And the none grating waveguide with the length L made a phase difference of π between the two modes at the resonant wavelength:

$$(\beta_{01}-\beta_{0m})L=(2M+1)\pi \tag{1}$$

where M is an integer. At the LPWG1 input port, only the fundamental mode is included, so the amplitude is A_{in} (B_{in} = 0), and the amplitudes at the LPWG2 output port are A_{out} and B_{out}. The mode transmission in the LPWG can be expressed as

$$\begin{bmatrix}A_{\mathrm{out}}\\B_{\mathrm{out}}\end{bmatrix}=\mathbf{T}_C^N\prod_{K=1}^{N-1}(\mathbf{T}_C^K\mathbf{T}_P^K)\begin{bmatrix}A_{\mathrm{in}}\\B_{\mathrm{in}}\end{bmatrix} \tag{2}$$

where N is the number of gratings in the LPWG, $\mathbf{T}_C^K$ is the mode coupling matrix, and $\mathbf{T}_P^K$ is the transmission matrix. The mode transmission in the no-LPG segment is

$$\begin{bmatrix}A_{\mathrm{out}}\\B_{\mathrm{out}}\end{bmatrix}=\exp(-\mathrm{j}\beta_{01}L)\begin{bmatrix}1&0\\0&\exp\{\mathrm{j}(\beta_{01}-\beta_{0m})L\}\end{bmatrix}\begin{bmatrix}A_{\mathrm{in}}\\B_{\mathrm{in}}\end{bmatrix}. \tag{3}$$

So the output of total structure is

$$\begin{bmatrix}A_{\mathrm{out}}\\B_{\mathrm{out}}\end{bmatrix}=\exp\{-\mathrm{j}\beta_{\mathrm{av}}(N_1+N_2-2)\Lambda-\mathrm{j}\beta L\}\times(-1)^{N_1+N_2-1}\begin{bmatrix}\cos\{C(N_1-N_2)\}A_{\mathrm{in}}\\\{\mathrm{j}\exp(\mathrm{j}\phi)\sin[C(N_1-N_2)]\}A_{\mathrm{in}}\end{bmatrix} \tag{4}$$

where N_1 and N_2 are the grating numbers of the LPWG1 and LPWG2, respectively. When CN_1 = $3\pi/4$ and CN_2 = $\pi/4$, both the LPWG1 and LPWG2 are equivalent to a 3 dB.

3. Designing and simulation

Based on this idea, the device structure what we finally fabricated is shown in Fig. 2. The input and output were composed of single-mode channel waveguides with a width of W_1. The middle part of the device was a multimode waveguide with a width of W_2, and two LPWGs were cascaded on the sidewall with a distance of L_s. The single-mode waveguides at the input and output ends and the multimode waveguide were connected by tapered transitions [12, 13].

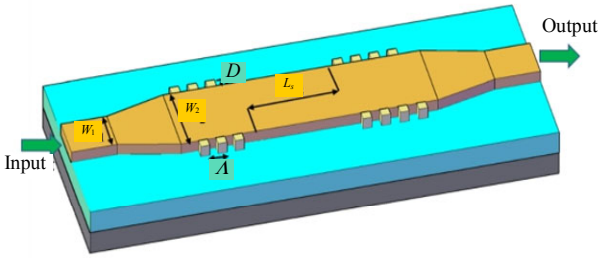

Fig. 2 Schematic diagram of the device structure.

The sidewall gratings supported the coupling between the E_{11} and E_{21} modes [14], which could increase the overlap between the two coupled modes and reduced the coupling length. Since the E_{21} mode is anti-symmetric, we designed an offset of $\Lambda/2$ for the grating on the left and right sidewalls.

We used polymer Epocore (n = 1.5715) as the core, polymer Epoclad (n = 1.5587) as the upper cladding, and SiO_2 as the lower cladding. Based on the effective index method and commercial model solving software COMSOL, the width of the multimode waveguide was 8.6 μm and the grating depth was 0.6 μm. The height and width of the single-mode waveguide were 7 μm and 4 μm, respectively. The thicknesses of upper and lower claddings were 15 μm and 13 μm, respectively.

The polarization of the mode was TE polarization by default, and the effective refractive index of the E_{11} mode was 1.5679, the effective refractive index of the E_{21} mode was 1.5636, and the grating period was 397 μm calculated according to the phase matching equation. When the incident wavelength was 1550 nm and the number of the first grating was fixed to be 6, as shown in Fig. 3(a), then we could couple about 52% of the E_{11} mode to the E_{21} mode, and the number of the second grating was also set to be 6, so that all energy in the E_{21} mode was coupled back to E_{11} mode.

The intermediate distance L_s should be set to enable a phase difference of π after the two working modes passed. From the relationship (1) between L_s and the propagation constants of the two working modes, we could get the relationship of the distance L_s between the two gratings periods:

$$L_s = \frac{2M+1}{2}\Lambda . \tag{5}$$

When the two modes passed the distance L_s, there would be a phase difference of π. We selected different grating pitches to verify the filtering effect of the device. The determined parameter was used to establish the device model in Rsoft. The simulated transmission spectrum is shown in Fig. 3.

The result showed that the cascade structure reduced the bandwidth of the filter by more than half, and the greater the distance between the two gratings (the larger M) was, the narrower bandwidth of the transmission spectrum stopband was. It was proved that the cascaded long-period sidewall waveguide grating was an effective method to achieve narrowband filters. So we selected M as 19 for experimental preparation.

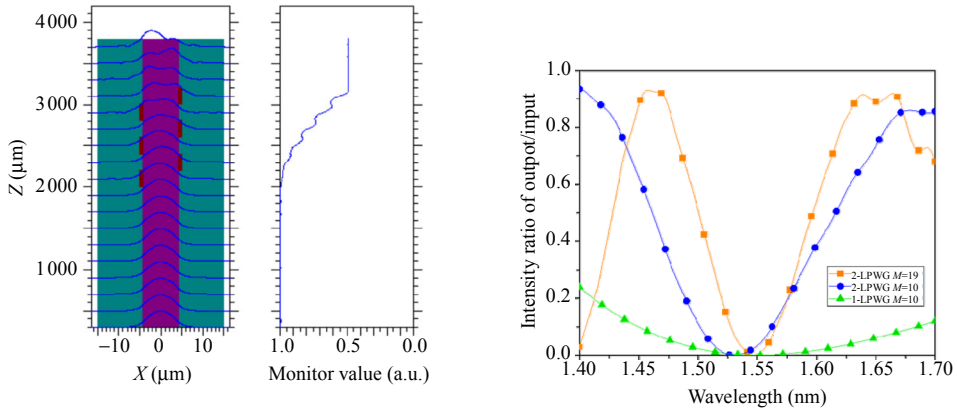

Fig. 3 Simulated transmission diagrams: (a) simulated conversion efficiency of the E_{11} mode to E_{21} mode at the first LPWG with 6 gratings and (b) simulated transmission spectrum. Single LPWG, M=10 (green line with triangle); cascaded-LPWGs, M=10 (blue line with circle); cascade-LPWGs, M=19 (orange line with square).

We fabricated the proposed device by using the standard photolithography process, as shown in Fig. 4. We first spin-coated a lower cladding on a Si substrate and then a core layer was spin-coated either. When the pattern of the core containing sidewall LPGs was formed by the photolithography process with the designed mask, an upper cladding was spin-coated.

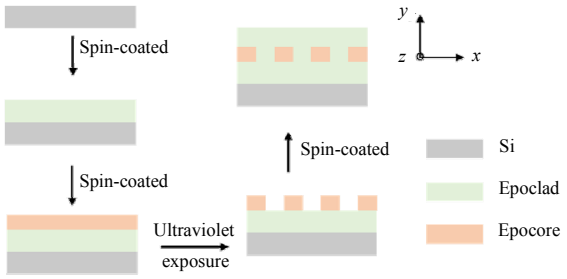

Fig. 4 Fabrication process.

4. Experimental results

The experimental setup was the same as our previous work in [15]. To characterize the fabricated device, the output light from a C+L-band amplified spontaneous emission source (ASE) (B&A Technology AS4600) was launched into the center of the access core through a single-mode fiber (SMF). The output light signal was collected via another SMF and monitored with an optical spectrum analyzer (OSA, Anritsu MS9740A). The first SMF was a lensed fiber and the second was a simple fiber. The sample pictures and microscope diagram of LWGs are shown in Fig. 5.

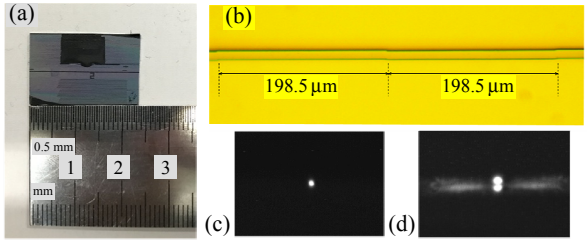

Fig. 5 Sample pictures and test spot: (a) fabricated sample picture, (b) diagram of LWGs under the microscope, and (c) and (d) are the test spot results of the E_{11} mode and the E_{21} mode, respectively.

From Figs. 5(c) and 5(d), we could get the great spot difference between the E_{11} mode and E_{21} mode. By slightly adjusting the relative position between the fibers and the device, we could observe the brightest circular spot, which meant that the E_{12} mode could not be excited or excited as little as possible, and then normalized transmission spectrum data under the highest light intensity were obtained on the spectrometer.

As shown in Fig. 6(a), it could be seen that the experimental transmission spectrum resonance wavelength was centered at 1577 nm, the extinction ratio of the device was 24 dB, and the 12 dB bandwidth was about 10 nm, which was almost the same as the simulation result in Rsoft in Fig. 6(b). The resonance wavelength was offset from the simulated resonance wavelength of 1 550 nm. Possible reasons include: the difference of the film thickness caused by uneven rotating coating of the glue machine, the difference of device temperature between the simulation and actual test, and the change of refractive index caused by device temperature and experimental time.

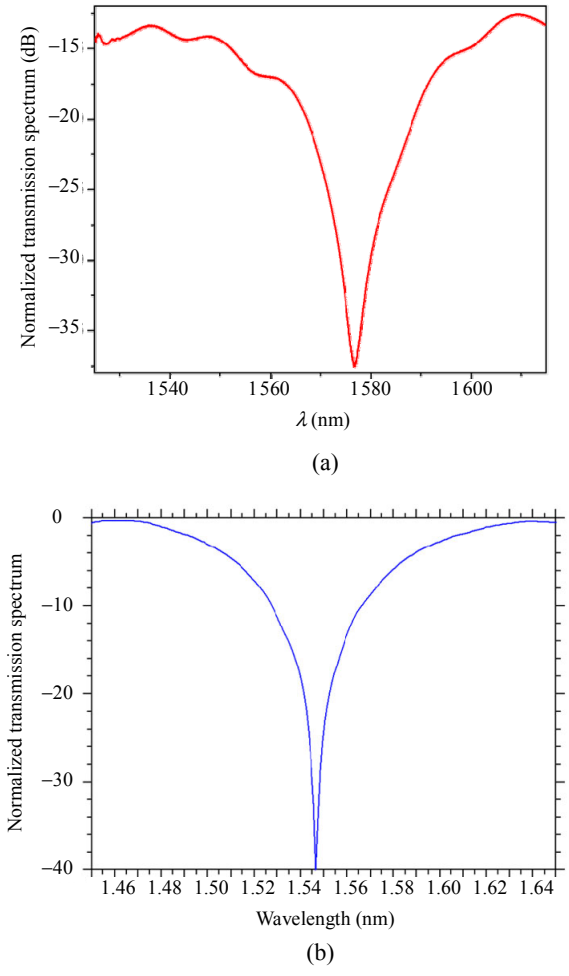

Fig. 6 Device transmission spectrum: (a) device transmission spectrum after experimental testing and data processing by origin and (b) simulated transmission spectrum by Rsoft.

The refractive indices of the waveguide material Epocore and Epoclad varied with temperature, so it would eventually cause the resonant wavelength of

the device shifting. We conducted experiments to test the temperature drift characteristics of the device. By changing the temperature of the heating plate, the corresponding output spectra were recorded from OSA, as shown in Fig. 7(a). It could be found that the resonant wavelength shifted to the long wavelength as the temperature rose, and the isolation of the stopband had basically been not changed.

The result of linear fitting to the obtained data is shown in Fig. 7(b). The temperature sensitivity of the filter was about 1.79 nm/℃. We could find that the resonant wavelength of the filter had a nearly linear response to the change of temperature, so we could achieve the purpose of tuning by changing the external temperature of the device.

Moreover, according to the previous analysis of L_s, as long as M was an arbitrary positive integer, no matter how the temperature changed, there must be a phase difference of π when the two working modes passed the length of L_s. Therefore, changing the temperature would only change the resonant wavelength and would not change the isolation of the transmission spectrum.

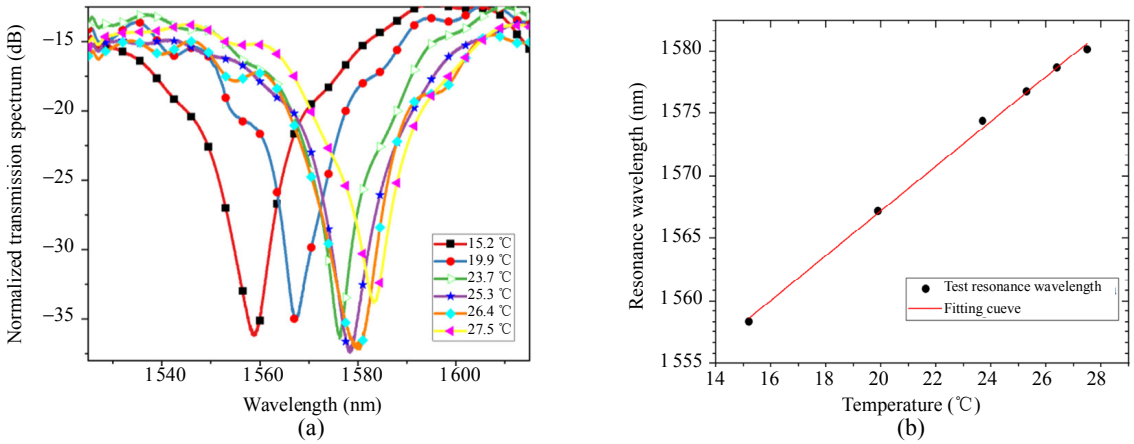

Fig. 7 Transmission spectrum of the fabricated device: (a) normalized transmission spectra at different temperatures and (b) fitting curve of temperature and central resonance wavelength.

5. Conclusions

In conclusion, we achieved a further increase in the filter bandwidth by cascading two polymer LPWGs. The experimental results showed that the device had a resonance wavelength at 1577 nm at room temperature and an isolation of 24 dB, with a 12 dB bandwidth of 10 nm. We obtained the temperature tuning characteristics of about 1.79 nm/℃. Compared with the fabrication process of microrings, the polymer waveguide process used in this study only needed to control the photolithography time to fabricate the waveguide, eliminating many technological requirements and enabling more flexible tuning by selecting different polymer materials. In addition, we could further reduce the size of the device by increasing the effective refractive index difference of the two operation modes and increasing the cascaded distance to achieve a narrower bandwidth.

References

[1] D. S. Starodubov, V. Grubsky, and J. Feinberg, “All-fiber bandpass filter with adjustable transmission using cladding-mode coupling,” *IEEE Photonics Technology Letters*, 1998, 10(11): 1590–1592.

[2] M. Partridge, S. W. James, J. Barrington, and R. P. Tatam, "Overwrite fabrication and tuning of long period gratings," *Optics Express*, 2016, 24(20): 22345–22356.

[3] X. Wang, Y. Wang, J. Flueckiger, R. Bojkoet, A. Liu, A. Reid, *et al*., "Precise control of the coupling coefficient through destructive interference in silicon waveguide Bragg gratings," *Optics Letters*, 2014, 39(19): 5519–5522.

[4] S. W. James and R. P. Tatam, "Optical fibre long-period grating sensors: characteristics and application," *Measurement Science & Technology*, 2003, 14(5): R49.

[5] W. K. Zhao, F. Feng, K. X. Chen, and K. S. Chiang "Reconfigurable broadband mode (de)multiplexer based on an integrated thermally induced long-period grating and asymmetric Y-junction," *Optics Letters*, 2018, 43(9): 2082–2085.

[6] W. Wang, J. Y. Wu, K. X. Chen, W. Jin, and K. S. Chiang, "Ultra-broadband mode converters based on length-apodized long-period waveguide gratings," *Optics Express*, 2017, 25(13): 14341–14350.

[7] Y. Yang, K. X. Chen, W. Jin, and K. S. Chiang, "Widely wavelength-tunable mode converter based on polymer waveguide grating," *IEEE Photonics Technology Letters*, 2015, 27(18): 1985–1988.

[8] L. Deng, D. Li, Z. Liu, Y. Meng, X. Guo, and Y. Tian, "Tunable optical filter using second-order micro-ring resonator," *Chinese Physics B*, 2017, 26(2): 024209.

[9] B. Wang, W. Zhang, Z. Bai, L. Wang, L. Zhang, Q. Zhou, *et al*., "CO2-laser-induced long period fiber gratings in few mode fibers," *IEEE Photonics Technology Letters*, 2014, 27(2): 145–148.

[10] Y. M. Chu, K. S. Chiang, and Q. Liu, "Widely tunable optical bandpass filter by use of polymer long-period waveguide gratings," *Applied Optics*, 2006, 45(12): 2755–2760.

[11] M. Sharma and S. Pal, "Design and analysis of nano-deep corrugated waveguide grating-based dual-resonant filters in visible and infrared regions," *Optik – International Journal for Light and Electron Optics*, 2013, 124(18): 3562–3566.

[12] Z. Tian, S. H. Yam, J. Barnes, W. Bock, P. Greig, J. M. Fraser, *et al*., "Refractive index sensing with Mach-Zehnder interferometer based on concatenating two single-mode fiber tapers," *IEEE Photonics Technology Letters*, 2008, 20(8): 626–628.

[13] S. Gross, N. Riesen, J. D. Love, and M. J. Withford, "Three-dimensional ultra-broadband integrated tapered mode multiplexers," *Laser & Photonics Review*, 2014, 8(5): L81–L85.

[14] W. Jin and K. S. Chiang, "Mode converter with sidewall-corrugated polymer waveguide grating," in *Opto-Electronics & Communications Conference,* Shanghai, 2015, pp. 1–3.

[15] R. Cao, L. Wang, and K. Chen, "Band-rejection filter based on cascaded two sidewall gratings in multimode polymer waveguide," in *Asia Communications and Photonics Conference*, Chengdu, 2019, pp. 1–3.